frontiers | Frontiers in Earth Science

ORIGINAL RESEARCH
published: 17 June 2022
doi: 10.3389/feart.2022.907967

High P-T Calcite-Aragonite Phase Transitions Under Hydrous and Anhydrous Conditions

*Xia Zhao[1,2], Zhi Zheng[1], Jiangzhi Chen[1], Yue Gao[1,2], Jianhui Sun[1], Xue Hou[1], Mengjun Xiong[1,2] and Shenghua Mei[1]**

[1]CAS Key Laboratory for Experimental Study Under Deep-Sea Extreme Conditions, Institute of Deep-Sea Science and Engineering, Chinese Academy of Sciences, Sanya, China, [2]University of Chinese Academy of Sciences, Beijing, China

The subduction of calcite into deep Earth and subsequent phase change are important for global carbon cycle. However, the study of the phase boundary between calcite and aragonite under high P-T conditions is insufficient due to sparse existing phase points and narrow pressure range. In addition, the impact of aqueous fluid on the phase transition requires further investigation. In this work, the calcite-aragonite phase transitions in both anhydrous and hydrous conditions were studied using diamond anvil cell (DAC) with *in-situ* Raman spectroscopy. In the anhydrous condition, investigations were conducted up to 12 GPa and 400°C and only the solid recrystallization-reconstructive (SRR) phase transition was observed. The calcite-aragonite boundary shows a convex upward curve with the minimum transformation temperature at around 150°C and a wide transformation pressure range from 1 to 12 GPa, consistent with the molar volume change between aragonite and calcite-I/II/III/IIIb. In the hydrous condition, both the SRR phase transition and dissolution-precipitation-dehydration (DPD) phase transition were observed under different heating conditions, and in the DPD phase transition ikaite serves as an intermediate phase precipitated from dissolved calcite and then dehydrates into aragonite. Our results suggest the phase transition of calcite-aragonite in the subduction zone, where the SRR phase transition can exist in slabs under wide P-T conditions (1–2 GPa and 160–400°C), and the DPD process can only occur under lower P-T conditions (less than 1.5 GPa and 110°C).

Keywords: calcite, aragonite, ikaite, phase transition, high P-T, Raman spectroscopy

Edited by:
Xi Liu,
Peking University, China

Reviewed by:
Zheng Haifei,
Peking University, China
Mingda Lv,
Argonne National Laboratory (DOE), United States
Sean Shieh,
University of Western Ontario, Canada

****Correspondence:***
Shenghua Mei
mei@idsse.ac.cn

Specialty section:
This article was submitted to Solid Earth Geophysics, a section of the journal Frontiers in Earth Science

Received: *30 March 2022*
Accepted: *12 May 2022*
Published: *17 June 2022*

Citation:
Zhao X, Zheng Z, Chen J, Gao Y, Sun J, Hou X, Xiong M and Mei S (2022) High P-T Calcite-Aragonite Phase Transitions Under Hydrous and Anhydrous Conditions. Front. Earth Sci. 10:907967. doi: 10.3389/feart.2022.907967

1 INTRODUCTION

Carbonate minerals, as the main carbon carriers, control carbon migration in different geochemical reservoirs (Dasgupta and Hirschmann, 2010; Merlini et al., 2012; Liu et al., 2017; Zhang Z. et al., 2018). Among them, calcite ($CaCO_3$) is the most common carbonate mineral. It is reported that calcite can exist at the top of the lower mantle (Wirth et al., 2009; Ague and Nicolescu, 2014; Kaminsky et al., 2016; Zhang Z.-W. et al., 2018; Lv et al., 2021), and under the mantle *P-T* conditions, it must adapt changes of pressure and temperature with depth and undergo significant phase changes (Suito et al., 2001; Hagiya et al., 2005; Merlini et al., 2012; Gavryushkin et al., 2017; Nestola et al., 2018; Hou et al., 2019). Understanding the $CaCO_3$ phase transitions and the structural properties of high *P-T* $CaCO_3$ phases is critical for predicting carbon states in deep Earth and their contributions to anomalies in the physicochemical parameters of subducting slab (Litasov and Ohtani, 2009;

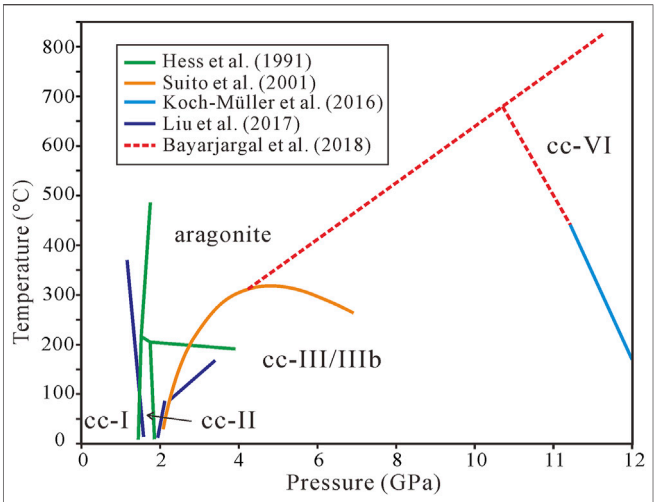

FIGURE 1 | The phase boundaries between calcite and aragonite from previous study. Under low pressures and temperatures, these boundaries are close, but they exhibit significant deviations for high pressures and temperatures.

Dasgupta and Hirschmann, 2010; Litasov et al., 2017; Yuan et al., 2021). Until now, more than 12 structural polymorphs, such as cc-I–VII (referred to as cc-I to cc-VII hereafter), aragonite, and pyroxene $CaCO_3$, have been verified (Maslen et al., 1993; Suito et al., 2001; Catalli and Williams, 2005; Hagiya et al., 2005; Ono et al., 2005; Oganov et al., 2006; Ono et al., 2007; Oganov et al., 2008; Merlini et al., 2012; Merlini et al., 2014; Gavryushkin et al., 2017; Li et al., 2018). Among various polymorphs of $CaCO_3$, the phase relationships among cc-I, cc-II, cc-III, and cc-VI have been well studied. However, the understanding of the phase boundary between calcite and aragonite at high *P–T* conditions is insufficient, and noteworthy discrepancy exists in previous works. Hess et al. (1991) obtained the phase boundaries among cc-I, cc-II, cc-III, and aragonite by Raman spectroscopy, and found that aragonite exists above 1.5 GPa and 150°C. Suito et al. (2001) performed XRD and Raman spectroscopy of the $CaCO_3$ phase transition and concluded that the boundary of cc-III and aragonite has a positive *P-T* slope in the pressure range 2–4.5 GPa followed by a negative *P-T* slope in the range of 4.5–6.2 GPa. Recently, Liu et al. (2017) obtained the transition temperature from calcite to aragonite increasing with pressure varying from 2.57 to 3.42 GPa according to Raman scattering measurements, consistent with Suito et al. (2001). These experiments (**Figure 1**) were based on very sparse phase points and narrow pressure ranges, leading to large uncertainty on the phase boundary. For a better understanding of the phase transitions of calcite under mantle conditions, we need to further investigate and clarify the phase relationship between calcite and aragonite.

Furthermore, due to dehydration of aqueous minerals (e.g., talcum, amphibole, brucite), the subduction zone is a place with plenty of water. Plummer and Busenberg (1982) and Morse and Mackenzie (1990) studied the solubility of $CaCO_3$ minerals and the aqueous speciation of carbon in great detail at ambient conditions and temperatures up to 90°C. Perdikouri et al. (2008) investigated the transformation of natural aragonite crystal to calcite by reaction with aqueous solutions of calcium carbonate at hydrothermal conditions for different periods of time, which indicated the replacement of aragonite by calcite followed an interface-coupled dissolution-precipitation mechanism. Yuan et al. (2021) found a dissolution-precipitation process between $CaCO_3$-I/II and aragonite phase transitions in hydrous fluids at *P-T* conditions lower than 1.5 GPa and 375°C and a solid recrystallization phase transition process at 1.7–1.8 GPa and 500–520°C. However, these studies neglect the role of aqueous fluid on phase transition between calcite and aragonite at higher pressure and more experimental conditions. Therefore, besides the study of phase boundaries, we also need to elucidate the impact of aqueous fluid.

In this study, the high *P-T* stability and behavior of $CaCO_3$ were investigated under both hydrous and anhydrous conditions using an externally heated Bassett-type DAC combined with the laser Raman and Fourier transform infrared (FTIR) spectroscopy technique. In the anhydrous condition, various Raman spectra of calcite polymorphs at high *P–T* conditions were collected, and the phase boundaries between cc-I, cc-II, cc-III, cc-VI, and aragonite were determined up to 12 GPa and 400°C. We used the Clausius–Clapeyron equation to analyze the thermodynamic significance of our experimentally determined phase boundaries. In the hydrous condition, two transition processes from calcite/aragonite to aragonite, i.e., solid recrystallization-reconstructive (SRR) phase transition and dissolution-precipitation-dehydration (DPD) process, were studied and the implications on plate subduction zone were discussed.

2 MATERIALS AND METHODS

Highly pure natural $CaCO_3$ crystals were used in all experiments. Ikaite was synthesized in water at 0.6–1 GPa, room temperature, with the original material of calcite or aragonite. High-pressure experiments for single-crystal calcite were performed at the CAS Key Laboratory for Experimental Studies under Deep-Sea Extreme Conditions, Institute of Deep-Sea Science and Engineering, Chinese Academy of Sciences (Sanya, Hainan, China). High pressure and high temperature are produced by an externally heated Bassett-type DAC (Bassett et al., 1993), in which nichrome wire heaters are wrapped around the seats and the two diamonds are externally heated to create a homogeneous temperature field in the pressure chamber by applying an electrical current. The temperature inside the sample chamber was the mean value measured by two K-type thermocouples (NiCr-NiSi) attached to the two diamond anvils. The temperature error is within 1°C. The DAC is equipped with two types of IIA low-fluorescence diamonds with a culet diameter of 300 μm. The DAC sample chamber has an ~100 μm diameter hole in the center of a rhenium gasket that was produced by a Drilex-2000 laser hole puncher. Water and a mixture of methanol and ethanol in a ratio of 4:1 were used as the pressure-transmitting medium. Pressure was determined by the fluorescence line of Y1 (617.8 nm) of Sm:YAG (Trots et al., 2013) or the ruby method (Mao and Bell, 1978).

Raman spectra of calcite and fluorescence spectra of ruby or Sm:YAG were collected by two spectrometers simultaneously to

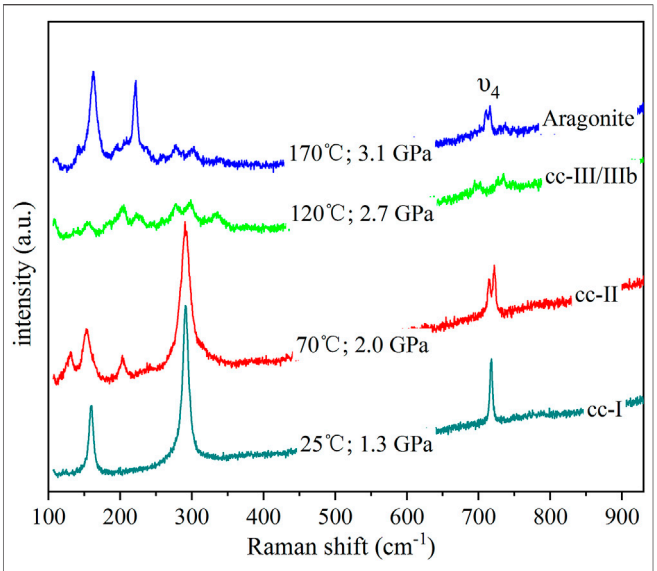

FIGURE 2 | Representative spectra from CD0061 at a certain pressure and temperature in an anhydrous condition.

ensure getting the real time pressure values. The Raman spectrum was collected from 100 to 930 cm^{-1} or 100 to 1200 cm^{-1}. The fluorescence spectrum was collected at approximately 617.8 or 694 nm. An Andor Shamrock SR500i spectrometer equipped with a Leica DM2700 microscope, a Plan Apo SL Infinity Corrected 20× objective with a numerical aperture value of 0.28, and a 532 nm frequency-doubled Nd: YAG laser. A 1800 or 1200 gr. mm^{-1} holographic grating coupled with a CCD detector (2000 × 256 ppi) with a spectral resolution of 1.5 or 3 cm^{-1} was used for the measurement of Raman spectra. The 1200 $gr.mm^{-1}$ holographic grating was used to measure fluorescence spectrum, which lead to ±0.23 and ±0.28 GPa of pressure error for ruby and Sm:YAG method. For all the Raman experiments, an externally heated Bassett-type DAC was first pressurized to the desired pressure, and then the sample chamber was heated (20°C/min) to the desired temperature. Raman and fluorescence spectra were simultaneously obtained after approximately 30 s at the desired condition to reach the equilibrium condition. Spectra were collected at a certain temperature and pressure interval to better understand the thermal stability of $CaCO_3$ at high pressure and high temperature.

To determine the influence of molecular water on phase transition in hydrous condition, FTIR spectra were collected using a Nicolet IS50 FTIR spectrophotometer (Thermo Fisher Scientific, China), equipped with a mercury cadmium telluride detector (MCT-A), a Continuμm microscope with 15× Reflachromat objective lens and a Ge-plated KBr beam splitter. Each sample was air-dried before measuring. Typically, 128 scans were recorded at a resolution of 4 cm^{-1} in the range of 700–4000 cm^{-1}. The frequency scale was internally calibrated by a helium-neon reference laser with an accuracy of 0.005 cm^{-1}. OMNIC software was used for spectra collection and manipulation. The three experiments used ultrapure water as pressure mediums were slowly heated to 460, 480, and 500°C. We kept the samples at their highest temperature for 20 min, and then quenched the samples to obtain FTIR spectra.

3 RESULTS AND DISCUSSION

3.1 Phase Transition in the Anhydrous Condition

For the anhydrous condition, mixed methanol and ethanol was used as the transmission medium. Representative Raman spectra are shown in **Figure 2**. Raman spectra of $CaCO_3$ can reveal different phases with distinctive structures (Koch-Mueller et al., 2016): cc-I is rhombohedral ($R\bar{3}c$), cc-II is monoclinic ($P2_1/c$) (Merrill and Bassett, 1975; Yuan et al., 2019), cc-III is less symmetrical than cc-II with triclinic ($P\bar{1}$) symmetry (Merlini et al., 2012), cc-VI crystallizes in the triclinic space group P1 (Bayarjargal et al., 2018), and aragonite has an orthorhombic structure of 2/m 2/m 2/m (Palaich et al., 2016). As shown in **Figure 2**, among 100–930 cm^{-1}, cc-I has three main peaks, including two external modes at about 160 and 280 cm^{-1}, and one υ_4 mode at about 720 cm^{-1}, whereas cc-II has four main peaks, including two external modes at about 150 and 280 cm^{-1}, and two υ_4 modes at about 720 cm^{-1}. Phases cc-III/IIIb can be distinguished from others based on the υ_4 modes, which have more than three peaks, and aragonite has four main peaks: two external modes at approximately 160 and 220 cm^{-1}, two υ_4 modes at about 720 cm^{-1}. All identified phases of the alcohol system are shown in **Figure 3**, showing five regimes: cc-I, cc-II, cc-III, cc-IIIb, and aragonite. The difference between cc-III and cc-IIIb has not been determined.

The dense phase points allow for much more accurate phase boundaries. In **Figure 3**, we observed that cc-I, cc-II, and cc-III/

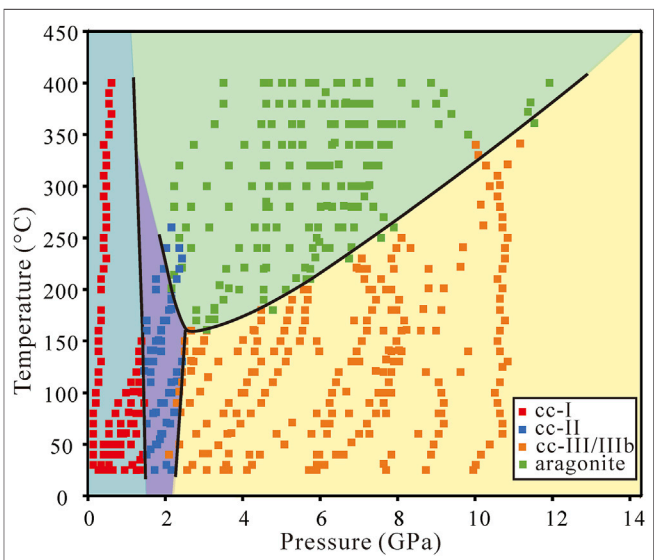

FIGURE 3 | Phase diagram of $CaCO_3$ in the anhydrous condition. The phase boundary between calcite and aragonite shows a minimum transition temperature at around 150°C and 2.4 GPa. Near each segment of the phase boundaries, there are some ambiguous points in which two phases can exist in a small vicinity, especially between cc-II and aragonite.

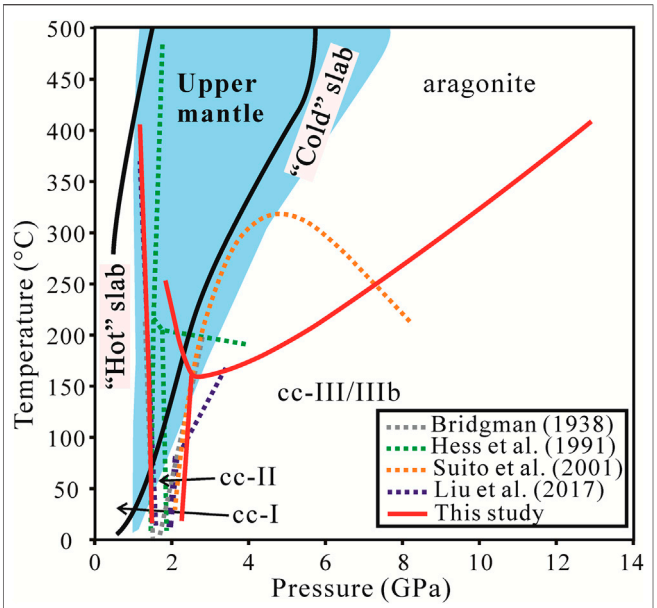

FIGURE 4 | Comparison of phase boundaries in different studies, with upper mantle and subducting plate conditions. The upper mantle is from Pan and Galli. (2016). The cold plate and the hot plate are from W1300 in Syracuse et al. (2010). At low pressures the deviations between our boundaries and previous works are relatively small, but at high *P-T* the boundaries are completely different.

IIIb can all transform directly to aragonite. The transformation from cc-I to cc-II and cc-II to cc-III occurs at about 1.7 and 2.2 GPa, with no significant temperature dependence. The calcite-aragonite boundary is a convex upward curve with the minimum transformation temperature at around 150°C and a wide transformation pressure range from 1 to 12 GPa. The transition temperature decreases with the pressure from 1.5 to 2.4 GPa, and above 2.4 GPa the transition temperature increases with the pressure.

The transformation from cc-I to cc-II is approximately 1.5 GPa (**Figure 4**), showing as an almost vertical line, consistent with Bridgman (1939), Hess et al. (1991), Suito et al. (2001), and Liu et al. (2017). According to the Clausius–Clapeyron equation,

$$dP/dT = L/(T\triangle V)$$

where P is the pressure, T is the temperature, L is the enthalpy change, and $\triangle V$ is the change of molar volume. The vertical phase boundary means $dP/dT \approx 0$, suggesting that the enthalpy from cc-I to cc-II is almost unchanged, and that the entropy change is very small.

The transformation pressure of cc-II to cc-III/IIIb is from 2.2 to 2.4 GPa (**Figure 4**) slightly different from Bridgman (1939), Hess et al. (1991), and Liu et al. (2017). This could result from the experimental condition and pressure error of different researches. The slopes for the phase boundaries of cc-II to cc-III/IIIb are positive with a high angle. Again, the Clausius–Clapeyron equation suggests a small enthalpy change when cc-II transforms to cc-III/IIIb.

TABLE 1 | Crystallographic data for calcite I-VI and aragonite. V_c is the value of the cell, and Z is the number of formula units in the unit cell.

Phase	Space Group	Z	V_c (Å^3)	Reference
$CaCO_3$	$R\bar{3}c$	6	368.07	Maslen et al. (1993)
$CaCO_3$- II	$P2_1/c$	4	239.57	Merrill and Bassett (1975)
$CaCO_3$- III	$P\bar{1}$	10	555.26	Merlini et al. (2012)
$CaCO_3$- III b	$P\bar{1}$	4	224.33	Merlini et al. (2012)
$CaCO_3$- VI	$P\bar{1}$	2	87.86	Merlini et al. (2012)
$CaCO_3$ aragonite	Pmcn	4	226.97	Negro and Ungaretti (1971)

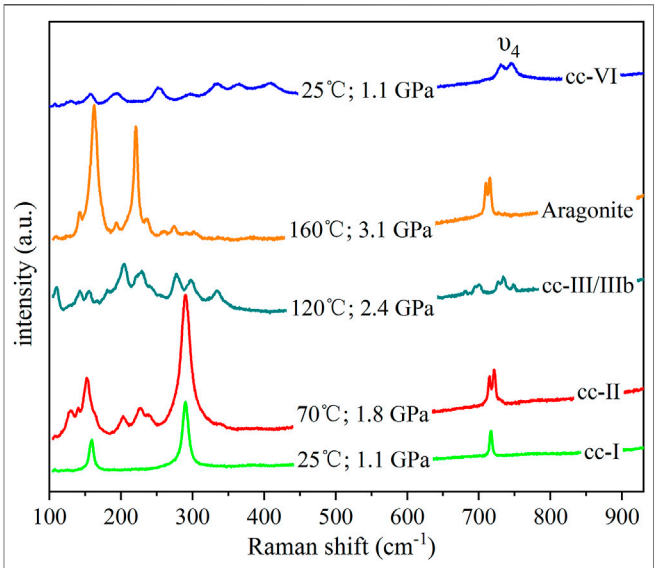

FIGURE 5 | Representative spectra from CD0036 (except cc-VI) at different pressures and temperatures in immediately heated up hydrous experiments. Cc-VI is from CD0054.

The transition temperature of calcite-aragonite decreases with pressure at low pressure from 1.5 to 2.4 GPa but increases with pressure at high pressure from 2.4 to 12 GPa (**Figure 4**). This is inconsistent with Bridgman (1939), Hess et al. (1991), and especially Suito et al. (2001). The phase boundaries are similar regardless of the water or alcohol system. From the thermodynamic perspective, the nearly-vertical phase boundaries between cc-I and cc-II, cc-II and cc-III/IIIb ensure that the enthalpy change between calcite and aragonite remains relatively unchanged, and the change in dP/dT slope can be easily explained by the change in molar volumes: the molar volume of cc-I, cc-II, cc-III, cc-IIIb, and aragonite was calculated as 36.93, 36.06, 33.43, 33.76, and 34.16 cm^3/mol from the crystallographic parameters V_c and Z in **Table 1** using

$$V_m = \frac{N_A V_c}{Z}$$

where N_A is the Avogadro constant. Given that the transition from calcite to aragonite is generally exothermic, i.e., $L > 0$, the sign of the slope dP/dT of the phase boundary will be negative for cc-I and cc-II to aragonite transition and positive for the cc-III/

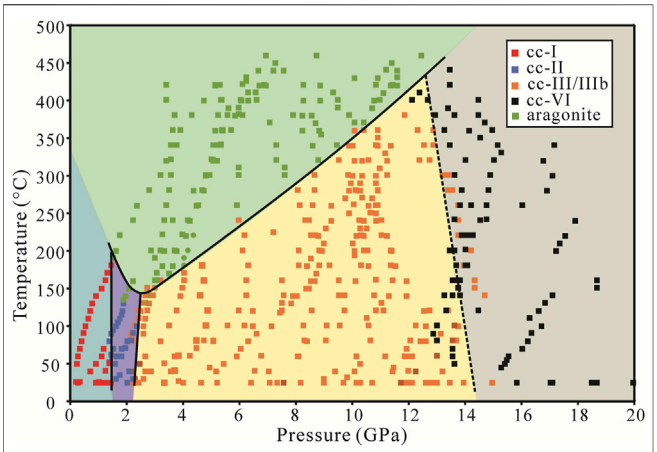

FIGURE 6 | Phase diagram of $CaCO_3$ in immediately heated-up hydrous experiments.

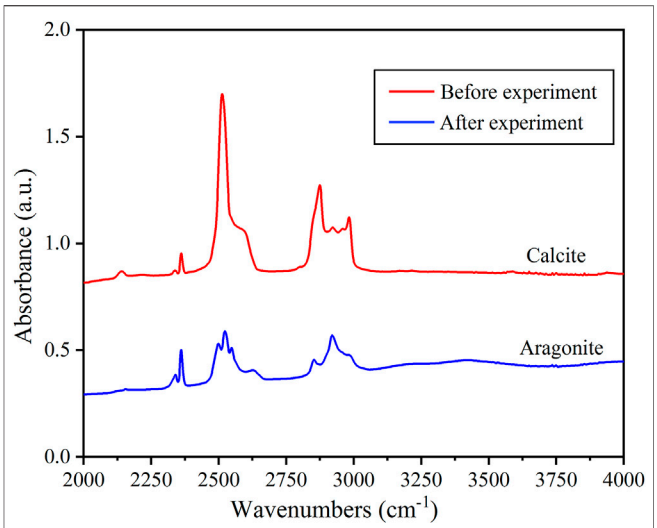

FIGURE 7 | Representative FTIR spectra for the three quenching samples before or after the experiment.

IIIb to aragonite transition. Suito et al. (2001), however, had a concave phase boundary between calcite and aragonite, possibly due to their sparse data points, that clearly contradicts the thermodynamics, and they had to resort to nonequilibrium kinetics as an explanation.

3.2 Phase Transition in the Hydrous Condition

In these experiments, calcite was heated up immediately after being loaded into the sample chamber. Ultrapure water was used as the transmission medium. The representative spectra at certain pressures and temperatures are shown in **Figure 5**. In addition to the Raman peak identification of each phase mentioned above, the cc-VI has many weak peaks in external modes and two main peaks in the υ_4 modes. All identified phases for the experiments in hydrous conditions are plotted in **Figure 6**, and we observed six regimes: cc-I, cc-II, cc-III, cc-IIIb, cc-VI, and aragonite. The phase boundaries among cc-I, cc-II, cc-III, cc-IIIb, and aragonite are similar to those in the anhydrous condition. Phase cc-VI was observed in this system, during the transformation from a low-pressure phase cc-III/IIIb to a high-temperature phase aragonite. The transition pressure from cc-VI to aragonite ranges from 13 to 15 GPa between 25 and 380°C. Because the phase boundary between cc-III/IIIb and cc-VI is less distinctive, it is not the focus of this study.

As mentioned in Zheng and Hermann (2014), when subducting to mantle depths, more molecular water can dissolve into nominally anhydrous minerals (NAMs) with increasing pressure. Because our experiments used ultrapure water as a pressure medium, it was possible that molecular water dissolved into calcite. To determine whether molecular water dissolved, we measured the water content of three quenched samples after the high-pressure and temperature experiments. FTIR spectra are the most widely used method to detect and analyze hydrous components (OH or H_2O) in minerals and glasses because of their high sensitivity and fast performance. It can identify a few to tens of ppm wt of H_2O in a mineral (Rossman, 2006). The FTIR spectra of free (gaseous) hydroxide and OH of mineral stretching frequency are adjacent but can be separated. Stretching vibrations of H_2O have broad bands at about 3248 and 3444 cm^{-1}. The FTIR spectra for the three quenched samples are almost the same as shown in **Figure 7**. The stretching vibration of OH for different minerals ranges from 3600 to 3700 cm $^{-1}$ (Zhang and Moxon, 2012). We used FTIR spectroscopy to measure the water content, and no signal of structured water, with a band at 3600–3700 cm^{-1}, was shown in **Figure 7**. Therefore, there was no dissolution of water in calcite for the three quenched samples. The phase boundaries of heated up immediately experiments in the hydrous environment (**Figure 6**) are similar to that in the anhydrous condition (**Figure 3**), indicating that the transformation from calcite to aragonite is an SRR process. Water plays the role of pressure-transmitting medium, which did not participate in the transformation process of calcite and aragonite.

3.3 Ikaite as an Intermediate Phase During Calcite Transition in the Hydrous Condition

Ikaite ($CaCO_3{\cdot}6H_2O$) is the hydrous form of calcium carbonate (Shahar et al., 2005), with a C2/c space group and $Z = 4$. Its structure contains discrete $CaCO_3$ ion pairs, each surrounded by 18 water molecules (Dickens and Brown, 1970). Pelouze (1831) was the first to synthesize $CaCO_3{\cdot}6H_2O$ in the laboratory, and Pauly (1963) discovered natural $CaCO_3{\cdot}6H_2O$ developing at the bottom of the Ika Fjord in Greenland, from which the name ikaite comes. In our experiments, we found that calcite transformed to ikaite after staying in the hydrous condition at 0.6–1 GPa and room temperature for hours. The formation conditions of ikaite in our experiments are consistent with Dickens and Brown (1970) and Van Valkenburg et al. (1971), where they found calcite and

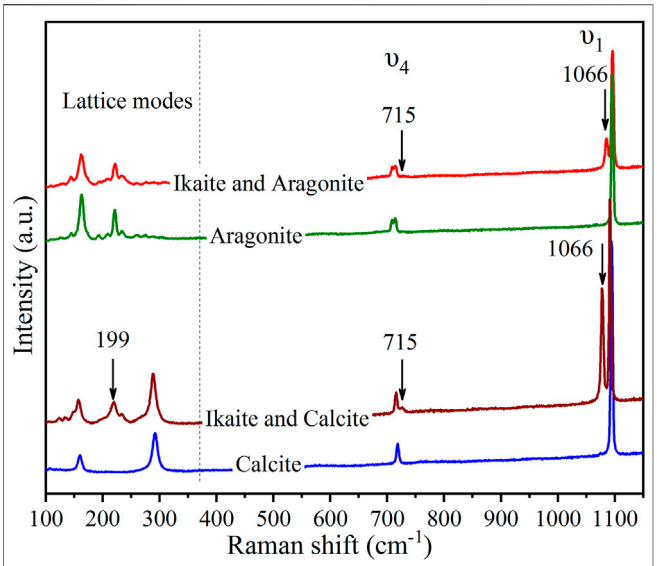

FIGURE 8 | Raman spectra of calcite, aragonite, and ikaite.

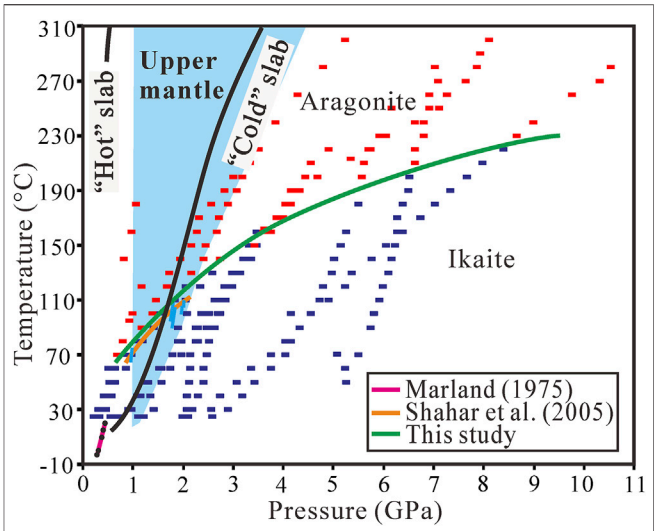

FIGURE 9 | The phase diagram of the transition of ikaite to aragonite extended to 9 GPa and 220°C.

aragonite become increasingly soluble in water as the pressure exceeds 0.6 GPa, and ikaite grows at the expense of both calcite and aragonite at pressures above 0.6–0.7 GPa.

Thus, we also investigate precipitated ikaite produced from dissolved calcite and aragonite in hydrous condition. The experiment process was similar with **Section 3.2**, expect that calcite stayed in an aqueous environment at room temperature and 0.6–1 GPa for hours to dissolve and precipitate as ikaite, and then started to be heated up. Ikaite has a spectrum similar to other calcium carbonate polymorphs (Rutt and Nicola, 1974; Long, 1977; Shahar et al., 2005), but they can be identified by the lattice modes υ_1 and υ_4. **Figure 8** compares the Raman spectra of calcite, aragonite, and ikaite. The main difference between aragonite and ikaite is the υ_1 mode, in which the peak of ikaite at 1066 cm^{-1} clearly distinguishes from aragonite, while cc-I and ikaite differ with the lattice modes υ_1 and υ_4, where the peaks of ikaite are at 199, 715, and 1066 cm^{-1}, consistent with Sánchez-Pastor et al. (2016).

In early work, Marland (1975) observed the transitions from ikaite to calcite/aragonite under very low *P-T* conditions (0.296–0.414 GPa and −2–14.3°C), and the phase diagram was extended to 2.5 GPa and 150°C by Shahar et al. (2005). In our work, we further extended the water saturated calcium carbonate phase diagram to 9 GPa and 220°C, shown in **Figure 9**. The phase boundary is consistent with Shahar et al. (2005) at a pressure below 2.5 GPa.

Calcite/aragonite first dissolved and then precipitated as ikaite, and subsequently dehydrated into aragonite when heated after staying at 0.6–1 GPa for hours, which is the DPD process. Compared to SRR, water molecules in DPD participate in the reaction process of transformation. Therefore, it can be concluded that different hydrous conditions in SRR and DPD processes lead to the distinction of the phase transition diagrams. Specifically, the phase boundary between calcite and aragonite in the SRR process is a convex upward curve with a minimum transformation temperature of around 150°C. It has a negative slope at 1.5–2.4 GPa and a positive slope at 2.4–12 GPa. While the ikaite-calcite boundary in DPD is a curve with a consistently positive slope, as the transition temperature increases with the increased pressure from 0.5 to 9 GPa. Additionally, at a certain pressure, the transition from ikaite to aragonite always occurs at a lower temperature compared to the calcite-aragonite phase transition.

3.4 Calcite to Aragonite Transition in Deep Earth

The Subduction zone is an area with plenty of aqueous fluid with some closed systems that don't contain water. When subducted into deep Earth, crystals in the oceanic slab will undergo hydrous or anhydrous phase transitions. Yuan et al. (2021) found two processes for calcite to aragonite transition in the hydrous system. One is the SRR phase transition, in which calcite transforms directly to aragonite, and the other is a dissolution-precipitation (DP) process, in which calcite dissolves and precipitates into aragonite.

In this paper, SRR is the only phase transition in the anhydrous system. As shown in **Figure 4**, the SRR phase transition can exist in both "hot" (i.e., high temperature low pressure) and "cold" (i.e., low temperature high pressure) slabs. During the subduction process, only cc-I and cc-II can transform to aragonite, and the transition occurs at *P-T* conditions at 1–2 GPa and 160–400°C. In the hydrous system, the phase diagram from the immediately heated experiments is an SRR phase transition, it can exist in both "hot" and "cold" slabs. On the contrary, the experiments heated after calcite/aragonite stayed at 0.6–1 GPa for hours is the DPD process. Thus, the DP process was not found in a hydrous system but SRR and DPD were observed instead. The DPD process needs ikaite as an intermediate phase, which can be formed in water at

0.6–1 GPa and room temperature or lower temperature and pressure conditions (Van Valkenburg et al., 1971; Marland, 1975; Shahar et al., 2005), but difficult to synthesize at higher pressure and temperature. As shown in **Figure 9**, the dehydration of ikaite into aragonite occurred under low *P-T* conditions (less than 1.5 GPa and 110°C). Therefore, in the subduction process, ikaite can only be dissolved and precipitated in a "cold" slab.

Aragonite is the main calcium carbonate in the deep upper mantle, which exists at more than 1 GPa and 100 °C according to the phase diagram (**Figures 4**, **9**). In both the hydrous and the anhydrous upper mantle, with pressure below 1.5 GPa, cc-I can exist in a temperature range of 25–400°C, and cc-II can exist at 1.5–2 GPa in a temperature range of 70–220°C. Ikaite can only be produced in the hydrous upper mantle under low *P-T* conditions (0.6–1 GPa and room temperature). But it can exist in 1–1.5 GPa at a temperature range of 40–100°C in the upper mantle.

4 CONCLUSION

We used DAC combined with Raman and FTIR spectra to study the phase diagram of the calcite to aragonite transition and the impact of aqueous fluid on this transition in this study. Two types of transmission media (water and alcohol) were used. In anhydrous system, the calcite to aragonite diagram was extended to 12 GPa and 400°C, with the calcite-aragonite boundary shown as a convex curve, which is consistent with the molar volume changes between the transition from aragonite to cc-III/IIIb and from aragonite to cc-I and cc-II. In the hydrous system, we observed two kinds of phase transformation mechanisms, the SRR phase transition, and the DPD process. The SRR occurred in an immediately heated process. It can exist in both "hot" and "cold" slabs, under high *P-T* conditions (1–2 GPa and 160–400°C) in the subduction zone. The DPD occurred in the system where calcite stayed at 0.6–1 GPa and room temperature for hours, then heated up. It can only occur on a "cold" slab under lower *P-T* conditions (less than 1.5 GPa and 110°C).

DATA AVAILABILITY STATEMENT

The original contributions presented in the study are included in the article/supplementary Materials, further inquiries can be directed to the corresponding author.

AUTHOR CONTRIBUTIONS

XZ, ZZ, JC, YG, and SM contributed to the conception and design of the study. XZ wrote the first draft of the manuscript and led the data analysis and interpreted the results with SM, XH, JS, and MX. All authors contributed to manuscript revision, read and approved it for publication.

FUNDING

This research was financially supported by Chinese Academy of Sciences (Grants Nos QYZDY-SSW-DQC029 and XDA22040501).

ACKNOWLEDGMENTS

We thank Junwei Li for his technical help on experiments.

REFERENCES

Ague, J. J., and Nicolescu, S. (2014). Carbon Dioxide Released from Subduction Zones by Fluid-Mediated Reactions. *Nat. Geosci.* 7, 355–360. doi:10.1038/ngeo2143

Bassett, W. A., Shen, A. H., Bucknum, M., and Chou, I. M. (1993). A New Diamond Anvil Cell for Hydrothermal Studies to 2.5 GPa and from −190 to 1200 °C. *Rev. Sci. Instrum.* 64, 2340–2345. doi:10.1063/1.1143931

Bayarjargal, L., Fruhner, C.-J., Schrodt, N., and Winkler, B. (2018). CaCO3 Phase Diagram Studied with Raman Spectroscopy at Pressures up to 50 GPa and High Temperatures and DFT Modeling. *Phys. Earth Planet. Interiors* 281, 31–45. doi:10.1016/j.pepi.2018.05.002

Bridgman, P. W. (1939). The High Pressure Behavior of Miscellaneous Minerals. *Am. J. Sci.* 237, 7–18.

Catalli, K., and Williams, Q. (2005). A High-Pressure Phase Transition of Calcite-III. *Am. Mineralogist* 90, 1679–1682. doi:10.2138/am.2005.1954

Dasgupta, R., and Hirschmann, M. M. (2010). The Deep Carbon Cycle and Melting in Earth's Interior. *Earth Planet. Sci. Lett.* 298, 1–13. doi:10.1016/j.epsl.2010.06.039

Dickens, B., and Brown, W. E. (1970). Crystal Structure of Calcium Carbonate Hexahydrate at about -120.Deg. *Inorg. Chem.* 9, 480–486. doi:10.1021/ic50085a010

Gavryushkin, P. N., Martirosyan, N. S., Inerbaev, T. M., Popov, Z. I., Rashchenko, S. V., Likhacheva, A. Y., et al. (2017). Aragonite-II and CaCO3-VII: New High-Pressure, High-Temperature Polymorphs of CaCO3. *Cryst. Growth & Des.* 17, 6291–6296. doi:10.1021/acs.cgd.7b00977

Hagiya, K., Matsui, M., Kimura, Y., and Akahama, Y. (2005). The Crystal Data and Stability of Calcite III at High Pressures Based on Single-Crystal X-Ray Experiments. *J. Mineralogical Petrological Sci.* 100, 31–36. doi:10.2465/jmps.100.31

Hess, N. J., Ghose, S., and Exarhos, G. J. (1991). "Raman Spectroscopy at Simultaneous High Pressure and Temperature: Phase Relations of CaCO3 and the Lattice Dynamics of the Calcite CaCO3(II) Phase Transition," in Proceedings XIII th AIRAPT international conference on high pressure science and technology, Oxford, New Delhi, 236–241.

Hou, M., Zhang, Q., Tao, R., Liu, H., Kono, Y., Mao, H.-K., et al. (2019). Temperature-induced Amorphization in CaCO3 at High Pressure and Implications for Recycled CaCO3 in Subduction Zones. *Nat. Commun.* 10, 1963. doi:10.1038/s41467-019-09742-5

Kaminsky, F., Matzel, J., Jacobsen, B., Hutcheon, I., and Wirth, R. (2016). Isotopic Fractionation of Oxygen and Carbon in Decomposed Lower-Mantle Inclusions in Diamond. *Min. Pet.* 110, 379–385. doi:10.1007/s00710-015-0401-7

Koch-Mueller, M., Jahn, S., Birkholz, N., Ritter, E., and Schade, U. (2016). Phase Transitions in the System CaCO3 at High P and T Determined by *In Situ* Vibrational Spectroscopy in Diamond Anvil Cells and First-Principles Simulations. *Phys. Chem. Minerals* 43, 545–561.

Li, X., Zhang, Z., Lin, J. F., Ni, H., Prakapenka, V. B., and Mao, Z. (2018). New High-Pressure Phase of CaCO 3 at the Topmost Lower Mantle: Implication for the Deep-Mantle Carbon Transportation. *Geophys. Res. Lett.* 45, 1355–1360. doi:10.1002/2017gl076536

Litasov, K. D., and Ohtani, E. (2009). Solidus and Phase Relations of Carbonated Peridotite in the System CaO-Al2O3-MgO-SiO2-Na2O-CO2 to the Lower

Mantle Depths. *Phys. Earth Planet. Interiors* 177, 46–58. doi:10.1016/j.pepi.2009.07.008

Litasov, K. D., Shatskiy, A., Gavryushkin, P. N., Bekhtenova, A. E., Dorogokupets, P. I., Danilov, B. S., et al. (2017). P-V-T Equation of State of CaCO 3 Aragonite to 29 GPa and 1673 K: *In Situ* X-Ray Diffraction Study. *Phys. Earth Planet. Interiors* 265, 82–91. doi:10.1016/j.pepi.2017.02.006

Liu, C., Zheng, H., and Wang, D. (2017). Raman Spectroscopic Study of Calcite III to Aragonite Transformation under High Pressure and High Temperature. *High Press. Res.* 37, 545–557. doi:10.1080/08957959.2017.1384824

Long, D. A. (1977). *Raman Spectropy*. New York City: McGraw-Hill, 276.

Lv, M., Dorfman, S. M., Badro, J., Borensztajn, S., Greenberg, E., and Prakapenka, V. B. (2021). Reversal of Carbonate-Silicate Cation Exchange in Cold Slabs in Earth's Lower Mantle. *Nat. Commun.* 12, 1712. doi:10.1038/s41467-021-21761-9

Mao, H. K., and Bell, P. M. (1978). High-Pressure Physics: Sustained Static Generation of 1.36 to 1.72 Megabars. *Science* 200, 1145–1147. doi:10.1126/science.200.4346.1145

Marland, G. (1975). The Stability of CaCO3·6H2O (Ikaite). *Geochimica Cosmochimica Acta* 39, 83–91. doi:10.1016/0016-7037(75)90186-6

Maslen, E. N., Streltsov, V. A., and Streltsova, N. R. (1993). X-ray Study of the Electron Density in Calcite, CaCO3. *Acta Crystallogr. Sect. B* 49, 636–641. doi:10.1107/s0108768193002575

Merlini, M., Crichton, W. A., Chantel, J., Guignard, J., and Poli, S. (2014). Evidence of Interspersed Co-existing CaCO3-III and CaCO3-IIIb Structures in Polycrystalline CaCO3 at High Pressure. *Mineral. Mag.* 78, 225–233. doi:10.1180/minmag.2014.078.2.01

Merlini, M., Hanfland, M., and Crichton, W. A. (2012). CaCO3-III and CaCO3-VI, High-Pressure Polymorphs of Calcite: Possible Host Structures for Carbon in the Earth's Mantle. *Earth Planet. Sci. Lett.* 333-334, 265–271. doi:10.1016/j.epsl.2012.04.036

Merrill, L., and Bassett, W. A. (1975). The Crystal Structure of CaCO3(II), a High-Pressure Metastable Phase of Calcium Carbonate. *Acta Crystallogr. Sect. B* 31, 343–349. doi:10.1107/s0567740875002774

Morse, J. W., and Mackenzie, F. T. (1990). *Geochemistry of Sedimentary Carbonates*. Amsterdam: Elsevier.

Negro, A. D., and Ungaretti, L. (1971). Refinement of the Crystal Structure of Aragonite. *Am. Mineralogist* 56, 768–772.

Nestola, F., Korolev, N., Kopylova, M., Rotiroti, N., Pearson, D. G., Pamato, M. G., et al. (2018). CaSiO3 Perovskite in Diamond Indicates the Recycling of Oceanic Crust into the Lower Mantle. *Nature* 555, 237–241. doi:10.1038/nature25972

Oganov, A. R., Glass, C. W., and Ono, S. (2006). High-pressure Phases of CaCO3: Crystal Structure Prediction and Experiment. *Earth Planet. Sci. Lett.* 241, 95–103. doi:10.1016/j.epsl.2005.10.014

Oganov, A. R., Ono, S., Ma, Y., Glass, C. W., and Garcia, A. (2008). Novel High-Pressure Structures of MgCO3, CaCO3 and CO2 and Their Role in Earth's Lower Mantle. *Earth Planet. Sci. Lett.* 273, 38–47. doi:10.1016/j.epsl.2008.06.005

Ono, S., Kikegawa, T., and Ohishi, Y. (2007). High-pressure Transition of CaCO3. *Am. Mineralogist* 92, 1246–1249. doi:10.2138/am.2007.2649

Ono, S., Kikegawa, T., Ohishi, Y., and Tsuchiya, J. (2005). Post-aragonite Phase Transformation in CaCO3 at 40 GPa. *Am. Mineralogist* 90, 667–671. doi:10.2138/am.2005.1610

Palaich, S. E. M., Heffern, R. A., Hanfland, M., Lausi, A., Kavner, A., Manning, C. E., et al. (2016). High-pressure Compressibility and Thermal Expansion of Aragonite. *Am. Mineralogist* 101, 1651–1658. doi:10.2138/am-2016-5528

Pan, D., and Galli, G. (2016). The Fate of Carbon Dioxide in Water-Rich Fluids under Extreme Conditions. *Sci. Adv.* 2, e1601278. doi:10.1126/sciadv.1601278

Pauly, H. (1963). *Ikaite, nyt mineral der danner skaer*. Copenhagen): Naturens Verden, 168–192.

Pelouze, J. (1831). Sur la production artifi cielle du carbonate de chaux cristallise,et sur deux combinaisons de ce sel avec l eau. *Ann. de Chimie de Physique* 2, 301–307.

Perdikouri, C., Kasioptas, A., Putnis, C. V., and Putnis, A. (2008). The Effect of Fluid Composition on the Mechanism of the Aragonite to Calcite Transition. *Mineral. Mag.* 72, 111–114. doi:10.1180/minmag.2008.072.1.111

Plummer, L. N., and Busenberg, E. (1982). The Solubilities of Calcite, Aragonite and Vaterite in CO2-H2O Solutions between 0 and 90°C, and an Evaluation of the Aqueous Model for the System CaCO3-CO2-H2O. *Geochimica Cosmochimica Acta* 46, 1011–1040. doi:10.1016/0016-7037(82)90056-4

Rossman, G. R. (2006). "1. Analytical Methods for Measuring Water in Nominally Anhydrous Minerals," in *Water in Nominally Anhydrous Minerals*. Editors H. Keppler and J. R. Smyth, 1–28. doi:10.1515/9781501509476-005

Rutt, H. N., and Nicola, J. H. (1974). Raman Spectra of Carbonates of Calcite Structure. *J. Phys. C. Solid State Phys.* 7, 4522–4528. doi:10.1088/0022-3719/7/24/015

Sánchez-Pastor, N., Oehlerich, M., Manuel, J., Melanie, A., and Christoph, K. (2016). Crystallization of Ikaite and its Pseudomorphic Transformation into Calcite: Raman Spectroscopy Evidence. *Geochimica Cosmochimica Acta* 175, 271–281. doi:10.1016/j.gca.2015.12.006

Shahar, A., Bassett, W. A., Mao, H. K., Chou, I., and Mao, W. (2005). The Stability and Raman Spectra of Ikaite, CaCO3{middle dot}6H2O, at High Pressure and Temperature. *Am. Mineralogist* 90, 1835–1839. doi:10.2138/am.2005.1783

Suito, K., Namba, J., Horikawa, T., Taniguchi, Y., Sakurai, N., Kobayashi, M., et al. (2001). Phase Relations of CaCO3at High Pressure and High Temperature. *Am. Mineralogist* 86, 997–1002. doi:10.2138/am-2001-8-906

Syracuse, E. M., Van Keken, P. E., Abers, G. A., Suetsugu, D., Bina, C., Inoue, T., et al. (2010). The Global Range of Subduction Zone Thermal Models. *Phys. Earth Planet. Interiors* 183, 73–90. doi:10.1016/j.pepi.2010.02.004

Trots, D. M., Kurnosov, A., Ballaran, T. B., Tkachev, S., Zhuravlev, K., Prakapenka, V., et al. (2013). The Sm:YAG Primary Fluorescence Pressure Scale. *J. Geophys. Res. Solid Earth* 118, 5805–5813. doi:10.1002/2013jb010519

Van Valkenburg, A., Mao, H. K., and Bell, P. M. (1971). Ikaite (CaCO3·6H,O), a Phase More Stable Than Calcite and Aragonite (CaCO3) at High Water Pressure. *Carnegie Inst. Geophye. Lab., Annu. Rep. Dir.* 1971, 233–237.

Wirth, R., Kaminsky, F., Matsyuk, S., and Schreiber, A. (2009). Unusual Micro- and Nano-Inclusions in Diamonds from the Juina Area, Brazil. *Earth Planet. Sci. Lett.* 286, 292–303. doi:10.1016/j.epsl.2009.06.043

Yuan, X., Gao, C., and Gao, J. (2019). An *In Situ* Study of the Phase Transitions Among CaCO3 High-Pressure Polymorphs. *MinMag* 83, 191–197. doi:10.1180/mgm.2018.140

Yuan, X., Mayanovic, R. A., and Zhang, G. (2021). Phase Transitions in CaCO3 under Hydrous and Anhydrous Conditions: Implications for the Structural Transformations of CaCO3 during Subduction Processes. *Am. Mineralogist* 106, 1780–1788. doi:10.2138/am-2021-7575

Zhang, M., and Moxon, T. (2012). *In Situ* infrared Spectroscopic Studies of OH, H2O and CO2 in Moganite at High Temperatures. *ejm* 24, 123–131. doi:10.1127/0935-1221/2011/0023-2165

Zhang, Z.-W., Wang, Y.-L., Qian, B., Liu, Y.-G., Zhang, D.-Y., Lü, P.-R., et al. (2018b). Metallogeny and Tectonomagmatic Setting of Ni-Cu Magmatic Sulfide Mineralization, Number I Shitoukengde Mafic-Ultramafic Complex, East Kunlun Orogenic Belt, NW China. *Ore Geol. Rev.* 96, 236–246. doi:10.1016/j.oregeorev.2018.04.027

Zhang, Z., Mao, Z., Liu, X., Zhang, Y., and Brodholt, J. (2018a). Stability and Reactions of CaCO3 Polymorphs in the Earth's Deep Mantle. *J. Geophys. Res. Solid Earth* 123, 10. doi:10.1002/2017jb015019

Zheng, Y.-F., and Hermann, J. (2014). Geochemistry of Continental Subduction-Zone Fluids. *Earth, Planets Space* 66, 93. doi:10.1186/1880-5981-66-93

Conflict of Interest: The authors declare that the research was conducted in the absence of any commercial or financial relationships that could be construed as a potential conflict of interest.